Handbook of Hemorheology and Hemodynamics
O.K. Baskurt et al. (Eds.)
IOS Press, 2007

© 2007 IOS Press. All rights reserved.

Blood Rheology Aspects of the Microcirculation

Herbert H. LIPOWSKY[1]
Department of Bioengineering
The Pennsylvania State University
University Park, PA 16802 USA

Introduction

To elucidate the basis for the drop in pressure from large artery to vein, Jean Léonard Marie Poiseuille (1797-1869) undertook a series of seminal studies that defined the laws of fluid flow in tubes of uniform cross-section and that identified the microcirculation as the major site of the resistance to flow [1, 2]. While best known for his meticulous experimental studies of viscous flow in glass tubes [2], he also made numerous observations in the mesentery of the frog and other microvascular preparations; these observations served to highlight the dynamics of red cell distribution, the presence of the annular plasma layer and the "skimming" of plasma by capillaries, and the adhesion of white cells to the endothelium of post-capillary venules [3]. Yet it wasn't until almost a century later that physiologists began to methodically explore the resistance to flow within the microcirculation proper using techniques of intravital microscopy. Landis [4] pioneered many quantitative methods for describing microvascular structure and function. Using finely drawn pipettes inserted into microvessels of frog mesentery, and calculating the velocity of bolus infusions of dyes through successive microvascular divisions, Landis attempted to calculate the resistance to flow within the capillary network and concluded that Poiseulle's law cannot be applied to the flow of blood through the capillary network except in a very limited sense. However, with the advent of sophisticated instruments for measurement of capillary pressure [5, 6] and red blood cell velocity [7], relatively precise quantitative measurements of pressure drops [8] and flow rates [9, 10] could be obtained; such measurements thus provided direct *in situ* flow resistance data for the hierarchy of microvessels from arteriole to venule [11].

As shown in Figure 1, measurements of pressure drops and flows in single unbranched microvessels [11] reveal that over the broad range of diameters (D) within the microcirculation proper, Poiseuille's fourth power relationship (i.e., resistance varies inversely with D^4) far overshadows other determinants of resistance in the normal flow state. The significance of this relationship cannot be understated in light of the fact that control and regulation of microvascular blood flow is manifest by the ability of the vascular system to alter resistance in response to vasomotor adjustments. However, striking departures from Poiseuille's relationship may dictate the outcome of

[1] *Corresponding author:* Department of Bioengineering, The Pennsylvania State Universit, University Park, PA 16802 USA; E mail: hhlbio@engr.psu.edu

PROOF

pathological flow states, with some examples including the low flow state, inflammation, and blood cell disorders. While the resistance to flow spans nearly five decades as blood courses its way from arteriole to venule, the large scatter in the experimental data may reflect significant departures from the flow of a Newtonian fluid through a smooth walled tube of circular cross-section. The effects of irregularities in geometry, broad variations in microvessel hematocrit and shear rates, blood cell deformability, red cell aggregation and blood cell adhesion to the endothelium are reviewed in the following.

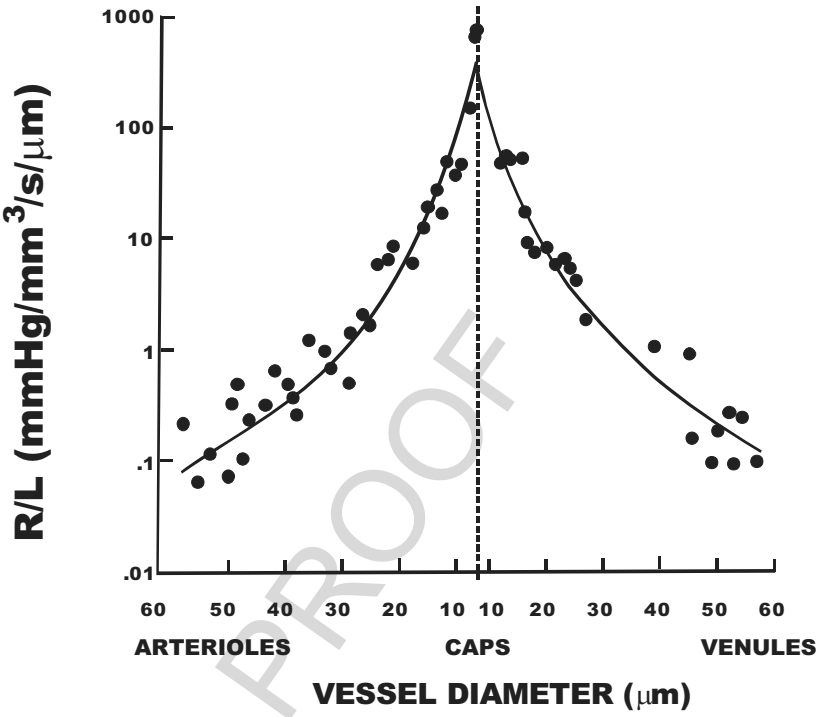

PROOF

Figure 1. Distribution of resistance per unit of vessel length (R/L) calculated for microvessels from direct in situ measurements of pressure drops and flows in intestinal mesentery. Power-law regressions (i.e., curved lines through data) reveal $R / L = (1.02 \times 10^{6})(D^{-4.04})$ for arterioles and $R / L = (1.07 \times 10^{6})(D^{-3.94})$ for venules. Redrawn from Lipowsky et al. [11].

1. In Vitro Foundations

Measurements of blood viscosity by bulk viscometry have emphasized the relative roles of shear rate, hematocrit, red cell aggregation and deformability in affecting blood flow in large vessels as well as establishing a framework for evaluating microcirculatory behavior [12]. With the use of tube, Couette and cone-plate viscometers and the calculation of an apparent viscosity as the ratio of shear stress divided by shear rate, *in vitro* studies have revealed that blood viscosity falls about 75% as shear rates ($\dot{\gamma}$) rise from ≈ 0.1 to 1000 s^{-1}. A comparison of this "shear thinning" of blood in the presence and absence of aggregating agents suggests that

about 75% of the decrease is a result of the disruption of red cell aggregates, and 25% is due to red cell deformation in response to increased shear stresses. At a given shear rate, blood viscosity rises exponentially with increasing red blood cell (RBC) volume fraction in the suspension (i.e., hematocrit), with the sensitivity dependent upon the prevailing $\dot{\gamma}$. The viscosity of the suspending medium in blood, termed plasma, has been shown to be Newtonian (i.e., invariant with $\dot{\gamma}$) and is dependent mainly upon protein content and temperature.

To relate bulk viscometry to blood behavior in tubes comparable in size to vessels of the microcirculation, numerous studies of flow in small bore tubes have provided a basis for understanding *in vivo* resistance to flow. The classical studies of Fåhraeus [13] demonstrating large reductions in tube hematocrit with diminishing tube diameter, and those of Fåhraeus and Lindqvist [14] showing concomitant reductions in the apparent viscosity of blood, have spawned many studies of blood viscosity in small bore tubes. In large part, these studies have been consistent with the relatively few direct *in vivo* measurements of apparent viscosity within single microvessels.

To illustrate, Figure 2 shows measurements of wall shear stress vs. shear rate obtained *in vitro* by Barbee and Cokelet [15] for a glass tube with nominal diameter of 29 μm (dashed line) and *in vivo* for a 34 μm diameter arteriole (solid line and data). *In vivo* values of wall shear stress (τ_{WALL}) were calculated from measurements of pressure drop (ΔP), vessel length (l) and diameter (D) [8], under the assumption of a vessel of uniform diameter and circular cross-section, and application of the principle of static equilibrium such that $\tau_{WALL} = \Delta P\, D / 4l$. *In vivo* and *in vitro* measurements are consistent with one another, although the *in vitro* measurements were made at substantially lower wall shear rates. *In vivo* measurements of shear stress at shear rates below 300 s^{-1} are typically much higher that those obtained *in vitro*, thus suggesting a greater increase in apparent viscosity with reductions in shear rate *in vivo* [11]. These *in vitro* studies also demonstrated that shear stress-shear rate relations for glass tubes of microvessel dimensions could be described regardless of tube size provided that the tube hematocrit was correctly specified. It was thus hypothesized that given the correct tube hematocrit, the relationship between blood viscosity and shear rates in microvessels could be uniquely specified for tubes representative of arterioles and venules. Because of the complexities of red cell distribution and heterogeneity of hematocrit within the microvascular network, this hypothesis has not been validated *in vivo*. However, at the low levels of microvessel hematocrit typical of the microcirculation, a nearly linear relationship between viscosity and tube hematocrit has been suggested by bulk viscometric measurements [16]. Direct measurements of pressure drops and flows in small arterioles (24 – 47μm diameter) have revealed a linear relationship between apparent viscosity and hematocrit when microvessel hematocrits were varied by intentional hemodilution with cell free plasma over a range of hematocrits from 3 – 35% [17]. This relationship was identical to that obtained by *in vitro* viscometry using a Weissenberg rheogoniometer at comparable shear rates of 2000 s^{-1}.

PROOF

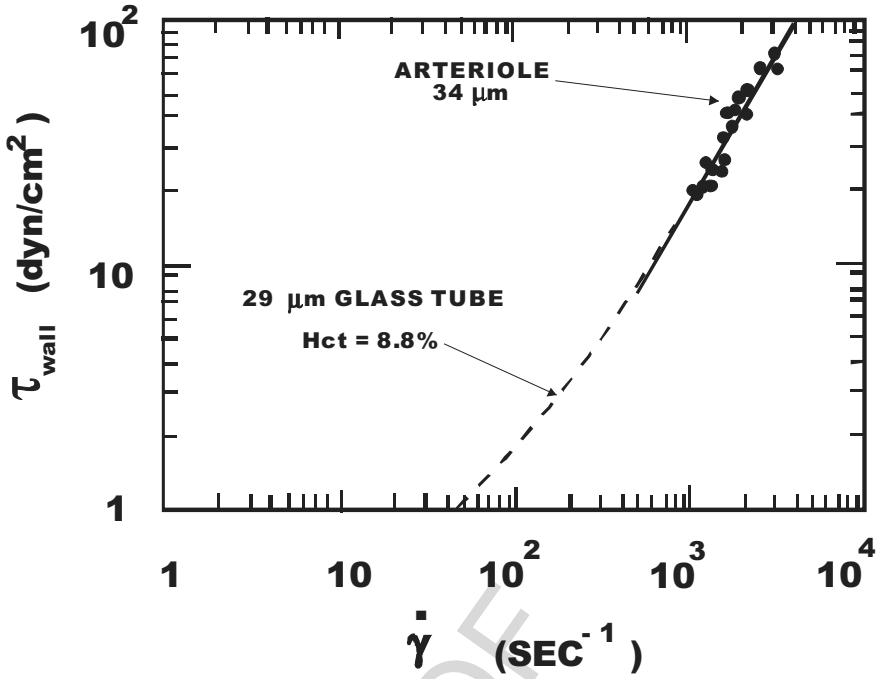

Figure 2. Comparison of wall shear stress (τ_{WALL}) vs shear rate (γ) for measurements in a 29 μm glass tube [15] with in vivo measurements for a small 34 μm arteriole [11].

With diminishing vessel diameter, the particulate nature of blood dominates the resistance to flow. *In vitro* simulation of capillary flows using polycarbonate sieves with 5 μm pores was pioneered by Gregersen, Chien and Usami [18] and emphasized the dominant contribution of red cell deformability to perfusion of capillaries. Through such experimental simulations it is now recognized that the initial deformation that red blood cells (RBC) and white blood cells (WBC) incur upon entry to a capillary contributes significantly to the pressure drop across individual capillaries [19-21]. Thus, the contribution of the intrinsic properties of blood to hemodynamic resistance changes markedly throughout the succession of vessels from arterioles to capillaries as diameter changes between divisions.

2. *In Vivo* Determinants of Blood Viscosity and Resistance

2.1. Blood Cell Deformability

The contribution of blood cell deformability to hemodynamic resistance varies markedly throughout the succession of vessels from arterioles to capillaries as diameter varies between divisions. Blood cell deformability affects the entrance of blood cells into capillaries and RBC with reduced deformability in pathological disorders (e.g., sickle cell disease) may be sequestered at the capillary entrance. Stiffening of the red cell membrane or elevations in hemoglobin viscosity may impede RBC transit through capillaries [22-24]. Studies of the flow of RBC with impaired deformability have been

PROOF

performed by infusing hardened cells into the subject animal and observing flow effects by intravital microscopy. For example, by hardening the RBC membrane with diamide and then infusing these cells into a rat, it was found that flow velocities in mesenteric capillaries were reduced by 30% under normal perfusion pressures and vascular stasis ensued following reductions in perfusion pressure[25]. Similar studies using RBC partially hardened with glutaraldehyde found that cells were preferentially sequestered in non-tube-like, sinusoidal vessels with preference for sequestration in bone marrow, liver, lung and spleen[26] .The normally stiffer WBC traverse the capillary network through larger thoroughfare channels [27], and WBC may become trapped at the capillary entrance or incur a prolonged transit time following their stiffening with activation during inflammation[28, 29].

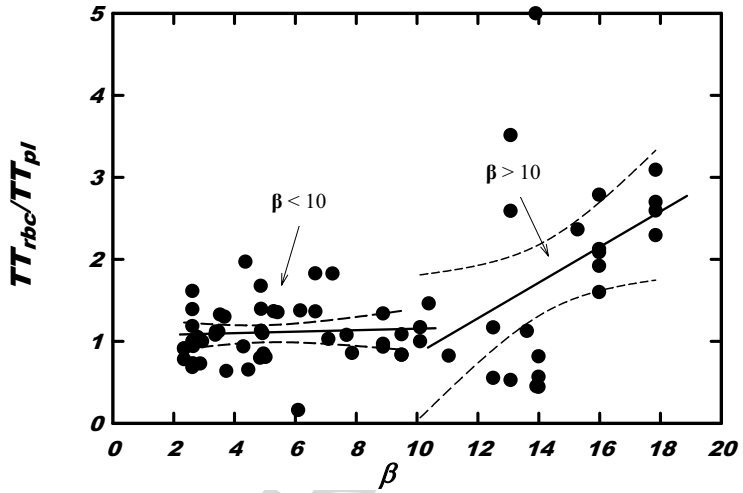

Figure 3. Mean Transit Time (TT) of hardened RBC relative to plasma for the transit from terminal arteriole to collecting venule across the capillary bed of cremaster muscle [30]. Prior to the infusion of bolus injections RBC deformability was measured by the steady state filtration method; the filtration parameter β was computed from the ratio of pressure drop across 5 μm filters for cells and suspending medium according to the method of Skalak et al. [31].

Use of the *in vitro* steady flow micropore filtration technique [18] to derive a quantitative assessment of cell deformability has placed *in vivo* observations on a firmer foundation. For example, using the deformability parameter, β, defined as the ratio of resistance to flow through a filter pore in the presence of red cells to that for suspending medium alone, it has been possible to understand how cell deformability affects RBC [30] and WBC [27] transit through the capillary bed. For example, shown in Figure 3 is the variation of the ratio of mean transit time of red cells through the capillary network in cremaster muscle, normalized to the mean transit time of plasma through the same vascular segment [30]. Transit time (TT) was computed from analysis of intensity-time curves following bolus injections of fluorescently labeled RBC or dextran dissolved in plasma. Intensity-time curves in terminal arterioles and collecting venules were recorded following bolus infusions of RBC hardened to various degrees with glutaraldehyde, with RBC deformability characterized by filtration. As shown, with increases in β from the norm of 2.4 up to 10.0, RBC traverse the capillary network with little hindrance and are able to recruit additional pathways through the capillary

network as needed. However, as β increases further, the transit time increases dramatically due to: (a) reductions in red cell velocity with increased rigidity; (b) reductions in the number of available parallel pathways due to sequestration of cells in the smallest diameter capillaries of the segment.

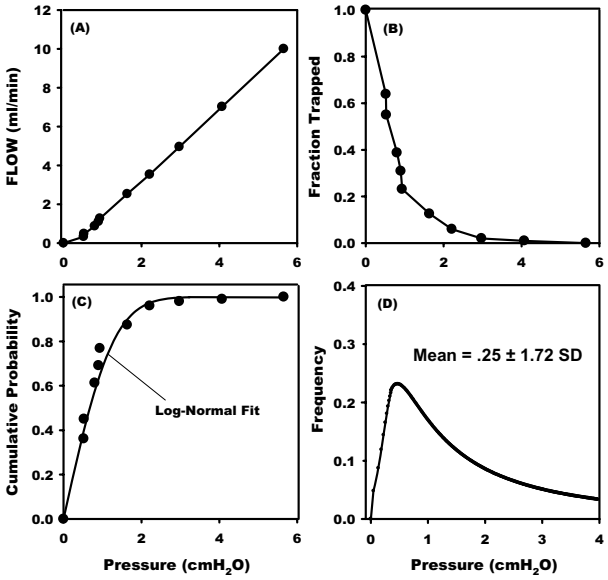

Figure 4. Transient filtration of leukocytes through 5 μm pore polycarbonate filters reveal the heterogeneity of cell deformability [35]. (A) A Bolus of WBC was initially trapped in the majority of pores in the filter and the flow steadily increased. (B) As pressure drop across the filter increased with flow, the fraction of cells trapped in pores decreased. (C) The cumulative probability of a cell passing through the filter at a given pressure drop was calculated as 1 – Fraction Trapped, and fit with a log-normal distribution. (D) Frequency distribution of yield pressures required to force a WBC through the pores.

While the steady state filtration technique provides a quantitative measure of cell deformability, it does not model the relationship between cell entrapment and the heterogeneity in size and deformability of the cell population. It has been shown that as flow rate increased through 5 μm pores of polycarbonate filters, the retention of WBC decreases exponentially with total flow through the filter [32]. In vivo studies of the sequestration of WBC in the pulmonary capillaries have shown that infused radiolabelled WBC exhibited an exponential washout with time that could be prolonged by hardening the WBC with glutaraldehyde prior to infusion [33]. Biophysical studies of the entry of WBC into micropipettes reveal that there exists a critical yield pressure (Py) which must be exceeded for a WBC of a given diameter to enter a micropipette of a specific size and that the independent geometric variable is the ratio of cell to pipette diameter [34]. To illustrate the effects of heterogeneity in cell deformability and diameter for a given population of WBC, and the heterogeneity of pore diameter in a polycarbonate filter, the transient filtration test was analyzed to determine a mean filtration pressure [35]. Shown in Figure 4A is the variation of total flow through a filter vs. pressure drop following the initial entrapment of a population of cells approximately equal in number to the total number of pores in the filter. As the

pressure drop increases from zero, flow initially increases non-linearly. The fraction of cells trapped at a given pressure (Figure 4B) was computed from the total number of pores and the resistance to flow ($\Delta P/Q$) measured during the washout of cells. Using this relationship to define the probability that a WBC remains trapped (p_r) for all pressures below the value on the abscissa, the probability that a cell will pass through the filter was then taken as $1-p_r$ and fit with a log-normal distribution (panel 4C). The probability density function that represents the frequency distribution of yield pressures, Py, was then computed (panel 4D). Under these idealized assumptions, it is evident that while the mean yield pressure is a relatively low value (i.e., mean = 0.25 cm H_2O), the standard deviation is relatively large and may represent the summated effects of heterogeneity in deformability as well as the ratio of cell to pore diameter.

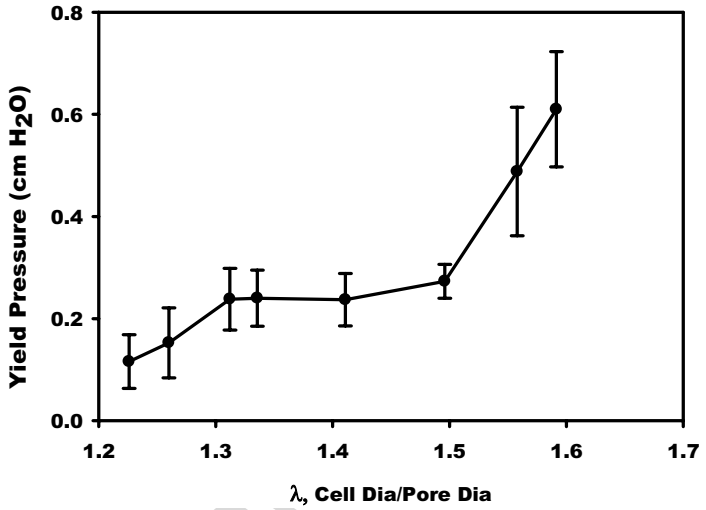

Figure 5. Mean yield pressure determined for a population of rat WBC as measured by the transient filtration method. The filter pores were enlarged by etching the filter in concentrated NaOH. The ratio of cell to pore diameter was calculated for the measured mean diameter of cells and filter pores; mean diameters determined by orifice-type electronic sizing and pore diameter via hydrodynamic analysis.

To assess the effect of varying pore diameter, polycarbonate micropore filters were etched with NaOH to enlarge the pores. The mean pore diameter (D_{PORE}) was then calculated from the measured pressure drop and flow of buffer through the filter, assuming Poiseuille's law holds for each of the measured total number of pores in the filter for a filter of known thickness (i.e., pore length). The mean cell diameter (D_{CELL}) of WBC in the suspension was determined using a Coulter counter calibrated against microspheres of known size. The resulting trends of mean yield pressure as a function of $\lambda = D_{CELL}/D_{PORE}$ are shown in Figure 5. Over the range of $1.3 \leq \lambda \leq 1.5$ there appears to be a relative plateau in mean yield pressure. This plateau appears to arise from the deformation of the WBC with greater pressure drops and flow rates through the filter as well as cells being swept through the pathways of least resistance (i.e., larger filter pores) at a given pressure drop. Such behavior has been noted *in vivo* as bolus infusions of WBC traverse the capillary network in cremaster muscle [27]. As shown in these muscle studies, WBC tend to take more centralized pathways through the

tissue via thoroughfare channels or the capillaries with the largest diameter. As λ increases above 1,5, a dramatic rise in the mean filtration pressure occurs, which is indicative of the propensity for cell sequestration with stiffened WBC during activation during the inflammatory process [27, 29, 36].

2.2. Red Cell Aggregation

The role of red cell aggregation (RCA) in affecting the resistance to flow in microvessels has not been fully clarified. Although *in vitro* viscometry demonstrates increases in blood viscosity with reductions in shear rate ($\dot{\gamma}$) [37], the resistance to flow in small-bore tubes does not necessarily exhibit the same correlation. *In vitro* studies with glass tubes comparable in size to microvessels [38] have suggested that the apparent viscosity of blood may decrease with onset of RCA, presumably because of exclusion of aggregates from the tube entrance or their radial migration toward the axial core of the tube. In contrast, direct *in vivo* hemodynamic measurements in normal [39] and low-flow states [40] reveal a dramatic rise in apparent viscosity and increased resistance with reductions in shear rate. It has been suggested that the behavior of aggregates at the entrance to successive arteriolar bifurcations and venular confluences may be a source of increased resistance to explain the basis for this disparity. It has also been postulated that the increased viscosity that arises from RCA may be negated by the migration of red cell aggregates to the central axial core of small vessels [41]. However, *in vivo* studies of the trajectories of red cell aggregates in venous vessels reveal that this effect is small and that a blunting of the velocity profile may be the dominant effect [41].

Analysis of the *in vivo* effect of RCA on resistance has been impeded by the inability to quantitatively define the degree of aggregation and the variability of aggregate strength obtained by different means. The use of high molecular weight dextrans (70–150 kDa) to induce RCA has been frequently used to induce RCA for studies of changes in flow and resistance [40-44]. *In vitro* and theoretical studies have provided a biophysical foundation for understanding the relationship between shearing forces and the strength of red cell aggregation. It has been shown that as the strength of aggregation increases, RBC form rouleaux and then clumps [45]. *In vivo* studies have demonstrated that the rouleaux are much more easily disrupted at bifurcations whereas clumps may become lodged at the entrance to capillaries [46]. A major problem with elucidating the effects of aggregation by direct intravital microscopy of the microcirculation has been that, as aggregation increases (e.g., dextran infusion), red cells become trapped in organs outside the field of view and hematocrit falls dramatically. Measurements of pressure drop from feeding arteriole (P_A) to collecting venule (P_V) in the modular network of rabbit omentum have shown that resistance, calculated from $\Delta P_{AV}/Q_{ARTERIOLE}$, first rises by about 10% as the circulating concentration of 500 kDa dextran increases to 1 gm%, then falls to 50% of normal as the concentration reaches 2 gm% [47]. This entrapment of cells in tissues outside the field of view suggests that the greatest influence of RCA is not its ability to increase blood viscosity, but rather its effect on cell sequestration at branch points in the microcirculation.

To illustrate the variability of hematocrit and aggregate formation observed in the microvasculature, Figures 6A and 6B show red cells flowing at reduced flow rate in post-capillary venules of rat mesentery. Induction of RCA by infusing fibrinogen into

PROOF

the systemic circulation of the rat, up to its maximum solubility of around 0.7 gm% which is the upper limit observed in clinical disorders, results in rouleaux formation in post-capillary venules during an induced low flow state. In contrast, the formation of clump-type RBC aggregates by infusion of 500 kDa dextran results in dramatic reductions in microvessel hematocrit. On average, microvessel hematocrit changed insignificantly due to fibrinogen but in response to dextran the packed cell fraction declined by almost 40% with a circulating concentration of 3 gm% [46, 48].

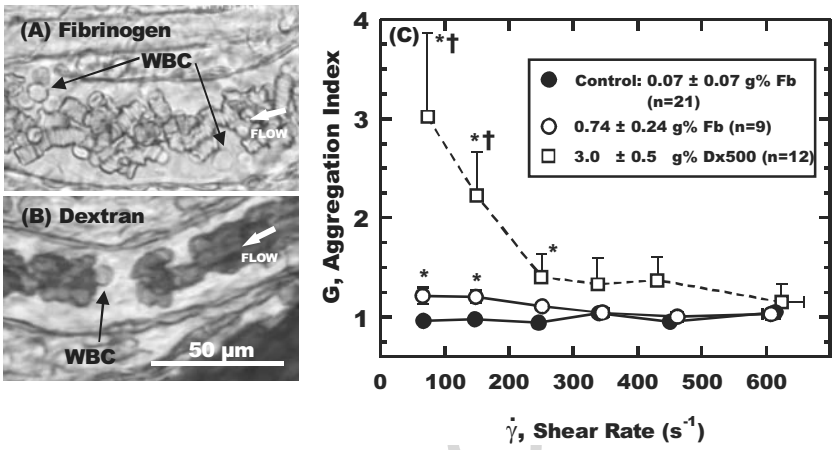

Figure 6. (A) Rouleaux formation of red cells in a post-capillary venule observed in the mesentery of the rat during reductions in flow achieved by upstream occlusion with a blunted micropipette for estimated wall shear rates < 50 s^{-1}. (B) Formation of clumped aggregates of red cells following infusion of 500 kDa dextran. (C) Aggregation index computed from light scattering measurements in post-capillary venules as a function of estimated wall shear rate, $\dot{\gamma}$, calculated from measured red cell velocity (V_{MEAN}) and vessel diameter (D) as $8V_{MEAN}/D$). Shear rates were reduced by a proximal occlusion of the feeding arterioles with a blunted micropipette. From [46] with permission.

Numerous techniques have been devised to quantitate red cell aggregation in a flow field, with applications to either in vitro flow models or direct microvascular measurements: estimates of aggregate size have been extracted from direct measurement of clump or aggregate size [44, 49], Fourier analysis of spatial variations in light intensity [50], analysis of transmitted and reflected light [51], and measurement of the light scattering properties of blood [48]. To illustrate the variability of RCA with shear rates in microvessels, Figure 6C presents an index of aggregation (G) computed from the light scattering of red blood cells [46]. The parameter G was computed from measurements of the scattering component of optical density, $OD_{SCAT.}$. Assuming that the effective size of a particle could be deduced from theoretical considerations of the relationship between OD_{SCAT} and the surface area to volume ratio of an aggregate, G then corresponds to the number of particles (i.e., individual red cells) per aggregate. With reductions in shear rates by occlusion of proximal microvessels, it appears that the dextran-induced aggregation is greater and more sensitive to shear rate compared with fibrinogen-induced aggregation. Observations of the disruption of aggregates at arteriolar to capillary bifurcations suggest that the rouleaux formed with fibrinogen are much more easily dispersed compared with the

clumps resulting from the 500 kDa dextran. In terms of hydrodynamics, the greatest difference between the two types of aggregation (i.e., fibrinogen vs. 500 kDa dextran) appears to be the effects on hematocrit and WBC margination. Although the fibrinogen-induced aggregation is much less in magnitude compared to dextran, the maintenance of a higher tube hematocrit with fibrinogen-induced RCA results in an enhanced radial migration of WBC and increased WBC flux along the venular wall [46]. In the case of dextran, the formation of large plasma gaps (Figure 6B) between aggregates tends to trap WBC and lessen their frequency of contact with the endothelium.

The effects of the intensity of aggregation and the size of aggregates on the resistance to flow remains to be explored. It has been postulated that disruption of aggregates as blood flows through microvessels having an irregular cross-section that varies with vessel length may cause an increase in energy dissipation [50]. This scenario has been implicated previously as a possible cause of the rise in measured effective viscosity of blood in arterioles and venules in response to reductions in shear rates [11]. Although aggregation measurements were not made in these studies, a four-fold increase in effective viscosity of blood was found in arterioles and venules with reductions in mean flow velocity from 4 to 0.2 mm/s. These large increases of *in vivo* viscosity were also attributed to the presence of leukocyte-endothelium adhesion, which affected the resistance to flow by obstructing the lumen. It was subsequently shown that when as few as 10 WBC adhere to the endothelium per 100 μm of vessel length in post-capillary venules, the resistance to flow may increase 2-fold [52]. The potential for enhanced WBC flux due to RCA may thus contribute to increased resistance to flow due to elevated WBC-endothelial cell adhesion.

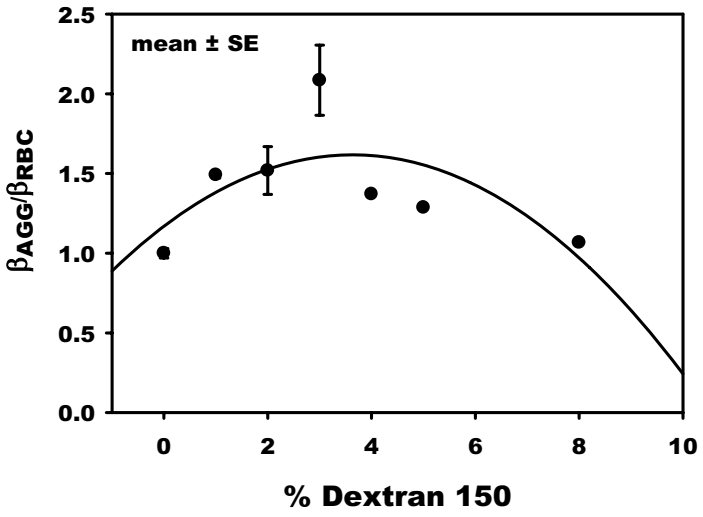

Figure 7. Steady state filtration test of red cell flow through 5μm pore polycarbonate filters. The filtration parameter β represents the ratio of the resistance to flow through a pore with red cells present to that with buffer alone [31] and is normalized to its value in a non-aggregating suspension (i.e., RBC in Ringers solution). Red cells from rat were suspended in Ringers solution containing the indicated concentration of 150 kDa dextran. The curve is a least squares quadratic fit of the data.

The effect of RCA on the ability of RBC to enter capillaries is also difficult to measure *in vivo*. However, in vitro tests using the steady state filtration method with 5

μm pore polycarbonate filters may provide new insights into abnormal increases in resistance attendant to RCA. Illustrated in Figure 7 are preliminary data for rat red cells resuspended in Ringers solution containing 150 kDa dextran. As shown, the steady state filtration parameter β (i.e., ratio of resistance to flow within a pore in the presence of RBC to resistance with buffer alone) increases by about 50% to a maximum at a concentration of dextran on the order of 3 gm%. If these relations apply *in vivo*, one would need a 50% increase of pressure gradient at the capillary level to maintain flow in capillaries.

2.3. Vascular Geometry

It must be emphasized that all rheological and flow measurements within the microvasculature are subject to the uncertainties associated with an imprecise knowledge of the vascular geometry. For example, when computing the effective viscosity of blood from measurements of pressure drop and flow it is assumed that the vessel is a smooth-walled cylinder of circular cross-section. Histological evidence clearly suggests otherwise. For example, many venules appear to be elliptical in cross-section, and this departure from the ideal is ignored when measuring venular diameter from observations of the width of a venule in the focal plane of a living tissue. Furthermore, normal vascular tone may change and the shape of the lumen may change dramatically with increased smooth muscle tone [53]. In previous studies measuring the *in vivo* apparent viscosity of blood in the microcirculation [11], it was found that the viscosity was 43% greater in venules compared to arterioles (5.15 vs 3.59 mPa.s, respectively). This disparity was attributed, in part, to irregularities in the microvessel walls, greater red cell aggregation due to the lower shear rates in venules, low levels of WBC-EC adhesion in the postcapillary venules and possibly unequal hematocrits.

To determine the errors incurred by neglecting irregularities in vascular diameter, studies have been performed to view the cross-section of venules in mesenteric tissue by using techniques of optical sectioning microscopy. By digitizing a stack of up to 50 images taken in 0.5 μm increments along the optical axis (i.e., z- direction), the luminal shape may be computed normal to the longitudinal axis of the vessel [54]. Shown in Figure 8 is the resulting cross-section of a post-capillary venule in a rat mesentery taken under fluorescence microscopy. The elliptical shape and other departures from a circular cross-section are clearly noted.

One can account for non-circular shapes in the measurement of flow resistance from Poiseuille's law by using the hydraulic diameter, D_H. The hydraulic diameter is defined as the diameter of an equivalent tube of circular cross-section that would have the same pressure drop for the same level of wall shear stress acting on tube or vessel walls having a wetted area S, and is defined by the relation: $D_H = 4A/S$, where A is the cross-sectional area of the vessel. For six venules ranging in width in the x-y focal plane from 9.0 to 23.0 μm with an average width of 17.5 ± 4.8 μm (mean ± SD), the average D_H was 15.9 ± 4.0 μm. Thus, due to the fourth power relationship between diameter and resistance given by Poiseuille's Law, the apparent 10% over estimation of luminal diameter using the width of the microvessel could result in a 40% overestimate of the apparent viscosity *in vivo*. The significance of these findings lies in the fact that earlier calculations of *in vivo* apparent viscosity [11] revealed a 50% greater apparent viscosity in postcapillary venules compared with arterioles in mesentery of the cat. Hence, given that arterioles are generally much more circular than venules in their non-vasoconstricted states [53], it is likely that irregularities in diameter may have played a

role in elevating the venular apparent viscosity. It would appear that a systematic analysis of the cross-sectional shape of small blood vessels is needed to fully understand resistance changes in normal and pathological flow states.

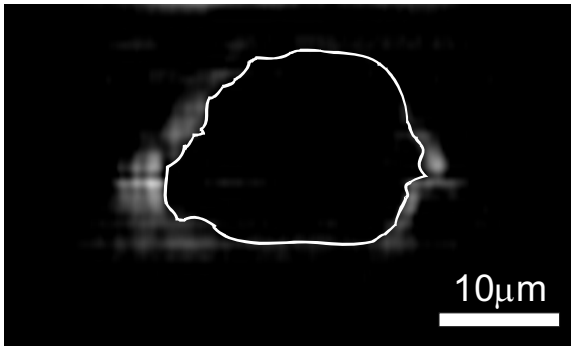

Figure 8. Computer reconstruction of the cross-section of a post-capillary venule in the mesentery of the rat. The venular endothelium was stained with the fluorescent dye acridine orange and a stack of 50 images digitized in the optical axis z- direction. The cross-section was computed by deconvolving the stack of x-y images using the techniques of optical sectioning microscopy [54]. The lumen of the vessel is outlined by the white line.

PROOF

In addition to these departures from the ideal, the presence of the macromolecular surface layer on the endothelium [55] has also been implicated as being hemodynamically significant [56]. The presence of a 0.3–1.0 μm thick layer (i.e., the glycocalyx) composed of proteoglycans and polysaccharides has been implicated as a significant source of increased resistance to flow in capillaries [56, 57]. Numerical simulations of blood flow through capillaries [58] suggest that red cell movement through a capillary may be hindered by the glycocalyx. Experimental measurements of the velocity profile within small venules suggest the presence of a significant displacement thickness due to the glycocalyx on the endothelium [59]. It has also been shown that the composition of the glycocalyx, and presumably its thickness, may be altered due to changes in wall shear stresses and/or enzymatic degradation during the inflammatory process [60]. The importance of these observations in affecting the resistance to flow in normal and pathological flow states remains to be explored.

3. Conclusions

The evolution of knowledge of the rheological behavior of blood flow in the microcirculation has provided a solid foundation for interpreting *in vivo* observations in normal and pathological flow states. The development of new instrumentation and approaches has paralleled the acquisition of rheological data and provided many new tools to bear on the problem. Many problems remain to be explored on both the cellular and molecular levels. The general approach to date has been to make observations at the cellular and/or molecular level and interpret them within the framework of a continuum (e.g., Poiseuille's law). However, with the advent of major advances in computational power, and new techniques of microscopy such as multi-photon spectroscopy or other fluorescence techniques, there is greater potential for addressing rheological questions at the molecular level and more completely

understanding the mechanics of microvascular perfusion. Such studies would facilitate the integration of the rheological properties of blood with mechanical forces that affect cell signaling events which, in turn, affect microvascular function in health and disease.

Acknowledgements

Supported by NIH-NHLBI Research Grant R01 HL39286.

References

[1] J.R. Pappenheimer**.** Contributions to microvascular research of Jean Leonard Marie Poiseuille. In: *APS Handbook on Microcirculation, Vol I.,* E.M.Renkin and C.C.Michel, Eds. 1984, pp. 1-10.
[2] S. Sutera and R. Skalak, The History of Poiseuille's Law, *Annu. Rev. Fluid Mech.* **25** (1993), 1-19.
[3] J.L.M. Poiseuille, Recherches sur les causes du mouvement du sang dans les vaisseaux capillaries., *C. R. Acad Sci.* **6** (1835), 554-560.
[4] E.M. Landis, Poiseulle's law and the capillary circulation., *Am. J. Physiol.* **103** (1933), 432-443.
[5] M. Intaglietta, R.F. Pawula and W.R. Tompkins, Pressure measurements in the mammalian microvasculature, *Microvasc. Res.* **2** (1970), 212-220.
[6] C.A. Wiederhielm, J.W. Woodburry, S. Kirk and R.F. Rushmer , Pulsatile pressures in the microcirculation of frog's mesentery, *Am. J. Physiol.* **207** (1964), 173-176.
[7] H. Wayland and P.C. Johnson, Erythrocyte velocity measurement in microvessels by a correlation method, *Bibl. Anat.* **9** (1967), 160-163.
[8] H.H. Lipowsky and B.W. Zweifach, Methods for the simultaneous measurement of pressure differentials and flow in single unbranched vessels of the microcirculation for rheological studies, *Microvasc. Res.* **14** (1977), 345-361.
[9] M. Baker and H. Wayland, On-line volume flow rate and velocity profile measurement for blood in microvessels, *Microvasc. Res.* **7** (1974), 131-143.
[10] H.H. Lipowsky and B.W. Zweifach, Application of the "two-slit" photometric technique to the measurement of microvascular volumetric flow rates, *Microvasc. Res.* **15** (1978), 93-101.
[11] H.H. Lipowsky, S. Kovalcheck and B.W. Zweifach, The distribution of blood rheological parameters in the microvasculature of cat mesentery, *Circ. Res.* **43** (1978), 738-749.
[12] S. Chien, S. Usami, J. Dellenback and V. Magazinovic, Blood rheology after hemorrhage and endotoxin, *Adv. Exp. Med. Biol.* **33** (1972), 75-93.
[13] R. Fahraeus, The suspension stability of blood, *Physiol. Rev.* **9** (1929), 241-274.
[14] R. Fahraeus and T. Lindqvist, The viscosity of blood in narrow capillary tubes., *Am. J. Physiol.* **96** (1931), 562-568.
[15] J.H. Barbee and G.R. Cokelet, Prediction of blood flow in tubes with diameters as small as 29 microns, *Microvasc. Res.* **3** (1971), 17-21.
[16] S. Usami, S. Chien and M.I. Gregersen, Viscometric characteristics of blood of the elephant, man, dog, sheep, and goat, *Am. J. Physiol.* **217** (1969), 884-890.
[17] H.H. Lipowsky, S. Usami and S. Chien, In vivo measurements of "apparent viscosity" and microvessel hematocrit in the mesentery of the cat, *Microvasc. Res.* **19** (1980), 297-319.
[18] M.I. Gregersen, C.A. Bryant, W.E. Hammerle, S. Usami and S. Chien, Flow Characteristics of Human Erythrocytes through Polycarbonate Sieves, *Science* **157** (1967), 825-827.
[19] R. Skalak, L. Soslowsky, E. Schmalzer, T. Impelluso and S. Chien, Theory of filtration of mixed blood suspensions, *Biorheology* **24** (1987), 35-52.
[20] P.S. Lingard, Capillary pore rheology of erythrocytes. 1. Hydroelastic behaviour of human erythrocytes, *Microvasc. Res.* **8** (1974), 53-63.
[21] G.W. Schmid-Schonbein, R. Skalak, S. Usami and S. Chien, Cell distribution in capillary networks, *Microvasc. Res.* **19** (1980), 18-44.
[22] T.S. Hakim, Effect of erythrocyte heat treatment on pulmonary vascular resistance, *Microvasc. Res.* **48** (1994), 13-25.
[23] D.K. Kaul and M.E. Fabry, In vivo studies of sickle red blood cells, *Microcirculation* **11** (2004), 153-165.
[24] K. Parthasarathi and H.H. Lipowsky, Capillary recruitment in response to tissue hypoxia and its dependence on red blood cell deformability, *Am. J. Physiol.* **277** (1999), H2145-H2157.

PROOF

[25] G.K. Driessen, T.M. Fischer, C.W. Haest, W. Inhoffen and H. Schmid-Schonbein, Flow behaviour of rigid red blood cells in the microcirculation, *Int. J. Microcirc. Clin. Exp.* **3** (1984), 197-210.
[26] S. Simchon, K.M. Jan and S. Chien, Influence of Reduced Red-Cell Deformability on Regional Blood-Flow, *Am. J. Physiol.* **253** (1987), H898-H903.
[27] M.J. Eppihimer and H.H. Lipowsky, Leukocyte sequestration in the microvasculature in normal and low flow states, *Am. J. Physiol* **267** (1994), H1122-H1134.
[28] M. Bathe, A. Shirai, C.M. Doerschuk and R.D. Kamm, Neutrophil transit times through pulmonary capillaries: the effects of capillary geometry and fMLP-stimulation, *Biophys. J.* **83** (2002), 1917-1933.
[29] A.G. Harris and T.C. Skalak, Effects of leukocyte capillary plugging in skeletal muscle ischemia-reperfusion injury, *Am. J. Physiol* **271** (1996), H2653-H2660.
[30] H.H. Lipowsky, L.E. Cram, W. Justice and M.J. Eppihimer, Effect of erythrocyte deformability on in vivo red cell transit time and hematocrit and their correlation with in vitro filterability, *Microvasc. Res.* **46** (1993), 43-64.
[31] R. Skalak, T. Impelluso, E.A. Schmalzer and S. Chien, Theoretical modeling of filtration of blood cell suspensions, *Biorheology* **20** (1983), 41-56.
[32] G.P. Downey and G.S. Worthen, Neutrophil retention in model capillaries: deformability, geometry, and hydrodynamic forces, *J Appl. Physiol* **65** (1988), 1861-1871.
[33] G.P. Downey, D.E. Doherty, B. Schwab, III, E.L. Elson, P.M. Henson and G.S. Worthen, Retention of leukocytes in capillaries: role of cell size and deformability, *J Appl. Physiol* **69** (1990), 1767-1778.
[34] E. Evans and A. Yeung, Apparent viscosity and cortical tension of blood granulocytes determined by micropipet aspiration, *Biophys. J.* **56** (1989), 151-160.
[35] M.J. Eppihimer and H.H. Lipowsky, The mean filtration pressure of leukocyte suspensions and its relation to the passage of leukocytes through nuclepore filters and capillary networks, *Microcirculation* **1** (1994), 237-250.
[36] M.J. Eppihimer and H.H. Lipowsky, Effects of leukocyte-capillary plugging on the resistance to flow in the microvasculature of cremaster muscle for normal and activated leukocytes, *Microvasc. Res.* **51** (1996), 187-201.
[37] Chien S. Biophysical behavior of red cells in suspensions. In: *The Red Blood Cell*, D.MacN Surgenor, Ed. New York: Academic Press, 1975, pp. 1031-1133.
[38] W. Reinke, P. Gaehtgens and P.C. Johnson, Blood viscosity in small tubes: effect of shear rate, aggregation, and sedimentation, *Am. J. Physiol* **253** (1987), H540-H547.
[39] G. Mchedlishvili, L. Gobejishvili and N. Beritashvili, Effect of intensified red blood cell aggregability on arterial pressure and mesenteric microcirculation, *Microvasc. Res.* **45** (1993), 233-242.
[40] M. Cabel, H.J. Meiselman, A.S. Popel and P.C. Johnson, Contribution of red blood cell aggregation to venous vascular resistance in skeletal muscle, *Am. J. Physiol* **272** (1997), H1020-H1032.
[41] P.C. Johnson, J.J. Bishop, S. Popel and M. Intaglietta, Effects of red cell aggregation on the venous microcirculation, *Biorheology* **36** (1999), 457-460.
[42] O.K. Baskurt and H.J. Meiselman, Blood rheology and hemodynamics, *Semin. Thromb. Hemost.* **29** (2003), 435-450.
[43] J.J. Bishop, A.S. Popel, M. Intaglietta and P.C. Johnson, Rheological effects of red blood cell aggregation in the venous network: a review of recent studies, *Biorheology* **38** (2001), 263-274.
[44] J.J. Bishop, P.R. Nance, A.S. Popel, M. Intaglietta and P.C. Johnson, Relationship between erythrocyte aggregate size and flow rate in skeletal muscle venules, *Am. J. Physiol.* **286** (2004), H113-H120.
[45] R. Skalak, P.R. Zarda, K.M. Jan and S. Chien, Mechanics of Rouleau formation, *Biophys. J.* **35** (1981), 771-781.
[46] M.J. Pearson and H.H. Lipowsky, Effect of fibrinogen on leukocyte margination and adhesion in postcapillary venules, *Microcirculation* **11** (2004), 295-306.
[47] H.H. Lipowsky, Microvascular rheology and hemodynamics, *Microcirculation* **12** (2005), 5-15.
[48] M.J. Pearson and H.H. Lipowsky, Influence of erythrocyte aggregation on leukocyte margination in postcapillary venules of rat mesentery, *Am. J. Physiol.* **279** (2000), H1460-H1471.
[49] S. Berliner, R. Ben Ami, D. Samocha-Bonet, S. Abu-Abeid, V. Schechner, Y. Beigel, I. Shapira, S. Yedgar and G. Barshtein, The degree of red blood cell aggregation on peripheral blood glass slides corresponds to inter-erythrocyte cohesive forces in laminar flow, *Thromb. Res.* **114** (2004), 37-44.
[50] K. Osterloh, P. Gaehtgens and A.R. Pries, Determination of microvascular flow pattern formation in vivo, *Am. J. Physiol.* **278** (2000), H1142-H1152.
[51] A. Gaspar-Rosas and G.B. Thurston, Erythrocyte aggregate rheology by transmitted and reflected light, *Biorheology* **25** (1988), 471-487.
[52] S.D. House and H.H. Lipowsky, Leukocyte-endothelium adhesion: microhemodynamics in mesentery of the cat, *Microvasc. Res.* **34** (1987), 363-379.
[53] J.E. Greensmith and B.R. Duling, Morphology of the constricted arteriolar wall: physiological implications, *Am. J. Physiol* **247** (1984), H687-H698.

PROOF

[54] Z. Shen and H.H. Lipowsky, Image enhancement of the in vivo leukocyte-endothelium contact zone using optical sectioning microscopy, *Ann. Biomed. Eng* **25** (1997), 521-535.
[55] A.R. Pries, T.W. Secomb and P. Gaehtgens, The endothelial surface layer, *Pflugers Arch.* **440** (2000), 653-666.
[56] A.R. Pries, T.W. Secomb, H. Jacobs, M. Sperandio, K. Osterloh and P. Gaehtgens, Microvascular blood flow resistance: role of endothelial surface layer, *Am. J. Physiol* **273** (1997), H2272-H2279.
[57] A.R. Pries and T.W. Secomb, Rheology of the microcirculation, *Clin. Hemorheol. Microcirc.* **29** (2003), 143-148.
[58] T.W. Secomb, R. Hsu and A.R. Pries, Motion of red blood cells in a capillary with an endothelial surface layer: effect of flow velocity, *Am. J. Physiol.* **281** (2001), H629-H636.
[59] E.R. Damiano, The effect of the endothelial-cell glycocalyx on the motion of red blood cells through capillaries, *Microvasc. Res.* **55** (1998), 77-91.
[60] A.W. Mulivor and H.H. Lipowsky, Inflammation- and ischemia-induced shedding of venular glycocalyx, *Am. J. Physiol.* **286** (2004), H1672-H1680.

PROOF